Current Research in Food Science 5 (2022) 1091–1097

Contents lists available at ScienceDirect

Current Research in Food Science

journal homepage: www.sciencedirect.com/journal/current-research-in-food-science

α-Glucosidase inhibitory activity of cannabidiol, tetrahydrocannabinol and standardized cannabinoid extracts from *Cannabis sativa*

Wiwit Suttithumsatid [a], Muhammad Ajmal Shah [b], Shabana Bibi [c,d], Pharkphoom Panichayupakaranant [a,e,*]

[a] Faculty of Pharmaceutical Sciences, Prince of Songkla University, Hat-Yai, 90112, Thailand
[b] Department of Pharmacy, Hazara University, Mansehra, Pakistan
[c] Department of Biosciences, Shifa Tameer-e-Millat University, Islamabad, Pakistan
[d] Yunnan Herbal Laboratory, College of Ecology and Environmental Sciences, Yunnan University, Kunming 650091, Yunnan, China
[e] Phytomedicine and Pharmaceutical Biotechnology Excellence Center, Faculty of Pharmaceutical Sciences, Prince of Songkla University, Hat-Yai, 90112, Thailand

ARTICLE INFO

Handling Editor: Alejandro G. Marangoni

Keywords:
α-Glucosidase
Cannabidiol
Cannabinoid
Cannabis
Diabetes mellitus
Tetrahydrocannabinol

ABSTRACT

Two major cannabinoids of cannabis, namely cannabidiol (CBD) and tetrahydrocannabinol (THC) have been reportedly used as alternative medicine for diabetes treatment in both pre-clinical and clinical research. However, their mechanisms of action still remain unclear. Therefore, this study aimed to evaluate the α-glucosidase inhibitory activity of THC, CBD and the standardized cannabinoid extracts. Based on *in silico* studies, THC generated hydrogen bonding and Van der Waals interactions, while CBD exhibited only Van der Waals interactions with functional residues of target α-glucosidase protein, with good binding energies of −7.5 and −6.9 kcal/mol, respectively. In addition, both of them showed excellent pharmacokinetic profiles with minor toxicity in terms of tumorigenic and reproductive effects. In addition, the enzyme based *in vitro* assay on α-glucosidase revealed that THC and CBD exhibited good inhibitory activity, with the IC_{50} values of 3.0 ± 0.37 and 5.5 ± 0.28 μg/ml, respectively. These were better than the standard drug, acarbose (IC_{50} of 488.6 ± 10.23 μg/ml). Furthermore, two standardized cannabinoid extracts, SCE-I (*C. sativa* leaf extract) and SCE-II (*C. sativa* inflorescence extract) exhibited stronger inhibitory activity than THC and CBD, with the IC_{50} values of 1.2 ± 0.62 and 0.16 ± 0.01 μg/ml, respectively. The present study provides the first evidence that the standardized cannabinoid extracts containing THC and CBD have greater potential than CBD and THC in application as an α-glucosidase inhibitor.

1. Introduction

Diabetes mellitus (DM) is a group of chronic disease characterized by abnormality of metabolic system, which leads to a high level of blood sugar. Hyperglycemia, a condition of excessive amounts glucose in the blood, is a common effect of DM. Extended period of uncontrolled hyperglycemia usually cause severe damage to many organs and tissue including nerves, and blood vessels (Galicia-Garcia et al., 2020). Over the last decade, prevalence of DM has been rapidly increasing and is now regarded as one of the most important global health issues. Approximately 460 million people or 6% of world population were affected by DM (Khan et al., 2020). Furthermore, DM was a top ten globally leading causes of death in 2019, and predicted to reach more than 500 million death in the next twenty-five years (Wu et al., 2021). DM can be managed by lifestyle/behavioral change and/or pharmacotherapeutic interventions. Presently, many classes of antidiabetic drugs are available including α-glucosidase inhibitors (Quattrocchi et al., 2020). The U.S. food and drug administration approves α-glucosidase inhibitors for treating type 2 DM patients as monotherapy or combined with other antidiabetic drugs in treatment regimen, especially in patients who have excessive postprandial glucose levels after consuming high-carbohydrate diets (Hossain et al., 2020).

α-Glucosidase is an important enzyme in the digestive system that is responsible for the digestion of carbohydrates into monosaccharides, such as glucose and fructose, allowing them to be absorbed into the bloodstream. Accordingly, the inhibition of α-glucosidase can reduce

* Corresponding author. Department of Pharmacognosy and Pharmaceutical Botany, Faculty of Pharmaceutical Sciences, Prince of Songkla University, Hat-Yai, 90112, Thailand.
E-mail address: pharkphoom.p@psu.ac.th (P. Panichayupakaranant).

https://doi.org/10.1016/j.crfs.2022.07.002
Received 20 April 2022; Received in revised form 28 May 2022; Accepted 1 July 2022
Available online 7 July 2022

carbohydrate digestion rate, lower glucose uptake, which result in lessened blood sugar level (DiNicolantonio et al., 2015; Alqahtani et al., 2020). However, many α-glucosidase inhibitor agents potentiate some disadvantages including gastrointestinal disturbances, causing of liver problem, and also contraindicate in patients who are at risk of diabetic ketoacidosis, inflammatory bowel disease, and colonic ulceration (Derosa and Maffioli, 2012).

Following the legalization of *Cannabis sativa* L., an annual herbaceous plant from the Cannabaceae family, for medical purposes in many countries, research interest in the biological and pharmacological properties of cannabis continue to rise. Furthermore, cannabinoids, a major and unique group of secondary metabolites found in cannabis, may play an important role in diabetes management (Suttithumsatid and Panichayupakaranant, 2020). Cannabidiol (CBD) and tetrahydrocannabinol (THC), the major cannabinoids commonly found in cannabis, may be the active compounds responsible for anti-diabetic effect due to their effect on the endocannabinoid system, which shares a numerous signaling pathway that maintains physiological stability and balancing many processes in the human body. However, detailed evaluation of their mechanisms of anti-diabetic effect is yet to be addressed (Horváth et al., 2012; Jadoon et al., 2016; Suttithumsatid and Panichayupakaranant, 2020). Cannabis leaves and inflorescences have been reported as the main sources of cannabinoids in cannabis plants due to abundant presence of glandular trichomes (Jin et al., 2020). In addition, leaves and inflorescences of cannabis are traditionally used as the main ingredients in the medical recipes (Crocq, 2020).

Although CBD has been recently reported to exhibit α-glucosidase inhibitory activity, *in silico* and *in vitro* (Ma et al., 2021), the effect of THC is still unknown. Therefore, the present study focused on comparison of α-glucosidase inhibitory effects of THC and CBD, both *in silico* and *in vitro*. Pharmacokinetic/ADMET profiles of THC and CBD were also determined, *in silico*.

Furthermore, the standardized cannabinoid extracts from the leaves and inflorescences were also investigated for their α-glucosidase inhibitory activity relative to the marker compounds, THC and CBD in order to determine the effect of their complexation of phytochemicals on α-glucosidase activity.

2. Materials and methods

2.1. Chemicals

CBD (98% purity) was purchased from Chemface, China. THC (99% purity) was prepared in-house according to our previous report submitted to Pharmaceutical and Biomedical Research Journal (in press). Dimethylsulfoxide (DMSO), ethanol and methanol (analytical grade) were obtained from RCI Labscan, Thailand. α-Glucosidase from *Saccharomyces cerevisiae* and *p*-nitrophenyl-α-D-glucopyranoside (pNPG) and acarbose were purchased from Sigma-Aldrich, USA. Dipotassium hydrogen phosphate, monopotassium phosphate, and sodium carbonate were obtained from Merck, Germany, Loba India, and Fluka, USA, respectively.

2.2. Plant materials

Inflorescences and leaves of *C. sativa* were obtained from Faculty of Natural Resources, Prince of Songkla University, Hat Yai Campus Thailand. The leaves and inflorescences were dried in a hot air oven at 60°C, for 24 h. The dried plant materials were then reduced to powder using an electric blender followed by sieving through a No. 20 sieve.

2.3. In silico experiment

2.3.1. Selection of target protein and cannabinoids

Three-dimensional structure of α-glucosidase macromolecule was downloaded from Protein databank (PDB) with accession ID: 5NN5 (Roig-Zamboni et al., 2017) and acquires resolution of 2.00 Å. Chemical structures of the selected cannabinoids, CBD (CID_644019) and THC, (CID_16078) were retrieved from PubChem database for further analysis (Kim et al., 2016).

2.3.2. Molecular docking method

The structures of CBD, THC and target protein (PDB ID: 5NN5) in pdb format were imported to the Autodock Vina software (Trott and Olson, 2010). Heteroatoms, 3D protonation, and water molecules along with the default ligand attached in the target molecules were removed. Number of polar hydrogens and Kollman charges were added to the selected ligand molecular structure for molecular docking analysis (Khan et al., 2022). Grid box dimensions with centers (x = −14.806, y = −29.611, z = 96.917) and sizes (x = 74, y = 70, z = 86) were generated using the selective residues. The active binding sites containing active residues of VAL193, PRO194, LEU195, GLU196, PHE490, THR491, LEU496, LEU565, LEU574, LEU577, THR578, ILE581, ARG585, ALA604, GLY605, ARG608, ARG696, LYS697, THR700, LEU701, ILE775, GLN776, VAL778, ILE780, GLU781, THR813, LUE814, and TYR609 were involved in the binding interactions with the selected ligand molecules. A reliable scoring scheme that resulted in the formation of binding energies of the best binding poses was established, and a number of molecular interactions, such as hydrogen bonding, Pi-bonding and hydrophobic interactions were retrieved by importing the docked complex to Discovery studio (D. Studio, Discovery Studio, Accelrys [2.1], 2008) visualization tool.

2.3.3. Determination of pharmacokinetic/ADMET profile

ADMET (absorption, distribution, metabolism, excretion, and toxicity) profiles of CBD and THC were determined to evaluate the drug-like attributes of the chemical compounds (Bibi and Sakata, 2017; Saleem et al., 2021a, 2021b). SwissADME (Daina et al., 2017) and Datawarrior tools (Sander et al., 2015) were used for the estimation of ADMET profiles of CBD and THC.

2.4. Preparation of standardized cannabinoid extracts

The dried powders of inflorescences and leaves were separately extracted using a microwave extraction. Briefly, the dried powders (2 g) were soaked in ethanol (20 ml) and placed in a microwave oven. The extraction was performed using a microwave power of 270 W, at 60–65 °C, for 1 min. After that, the extracts were filtrated through a filter paper and subjected to solvent evaporation using a rotary evaporator, at 50 °C to produce *C. sativa* leaf (SCE-I) and inflorescence (SCE-II) extracts. The dried extracts were subjected to quantitative HPLC determination of CBD and THC.

2.5. Quantitative HPLC determination of CBD and THC

Quantitative HPLC determination of CBD and THC in the extracts was performed using a method previously described (Saingam and Sakunpak, 2018), with some modifications. The method was performed using a UFLC Shimadzu model equipped with a photodiode-array detector and autosampler (Shimadzu Corp. Kyoto, Japan). A Luna® C18 column 4.6 mm × 250 mm, 5 μm (Phenomenex, Thailand) was eluted with a mobile phase consisted of methanol and water (85:15, v/v) at a flow rate of 1 ml/min. Monitoring of CBD and THC was performed using a UV–Vis spectrophotometer at 220 nm. The injection volume was 20 μl. All experiments were performed in triplicate. Calibration curves of CBD and THC were established using the authentic compounds at six concentrations between 6.25 and 200 μg/ml. Based on the linear regression, the calibration curves of CBD and THC were $Y = 72615X + 72146$ ($r^2 = 0.9998$) and $Y = 54467X + 77267$ ($r^2 = 0.9999$), respectively.

2.6. α-Glucosidase inhibition assay

α-Glucosidase inhibitory activity was determined using a method previously described (Shah et al., 2017), with some modifications. Concisely, α-glucosidase enzyme (0.1 Unit/ml) was dissolved in 0.1 M potassium phosphate buffer (pH 6.8). The samples were dissolved in DMSO (the final concentration of DMSO did not exceed 7%). Subsequently, 20 μl of each sample was mixed with 20 μl of enzyme solution in a 96-well microtiter plate, then incubated at 37 °C for 10 min. After that, pNPG (40 μl) was added, and the mixture was further incubated at 37 °C for 40 min. After incubation, 0.2 mM sodium carbonate in phosphate buffer (80 μl) was added to each well to stop the reaction. The amount of final product (*p*-nitrophenol) was measured using a microplate reader at 405 nm. The blank control was performed by the same protocol, but the α-glucosidase enzyme solution was replaced with the boiled enzyme. The control experiment also performed with the same process, but the sample solution was replaced with the same concentration of DMSO and deionized water in the sample solution. Acarbose was used as a positive control. The experiments were carried out in triplicate. The percentage inhibition was calculated using the following equation:

$$\%\text{Inhibition} = [(\text{Ac-Ab}) - (\text{As-Ab})] / (\text{Ac-Ab}) \times 100$$

Where: Ac = Absorbance of control, As = Absorbance of sample, Ab = Absorbance of blank.

2.7. Statical analysis

The results are expressed as mean ± SD. Statistical significance was calculated using one-way analysis of variance (ANOVA) followed by Tukey's multiple range test ($p < 0.05$).

3. Results and discussion

3.1. In silico studies

3.1.1. Molecular docking

Molecular docking is an appropriate molecular modeling application, explaining significant scoring scheme, and best binding poses generated by best docked complex. This assist in the retrieval of protein-ligand binding interaction; hence, it could be helpful in understanding the molecular mechanism of bounded ligand in the vicinity of the active site of target protein (Fathima and Murugaboopathi, 2019; Khan et al., 2021). Previous studies has proved that this is a powerful tool and very significant method in computer-aided drug design and development procedures to explain the molecular mechanism of bounded ligand with target protein/receptors, thus facilitating the identification of several bioactive compounds against many diseases (Ismail et al., 2021; Saleem et al., 2021a, 2021b). Based on a molecular docking analysis against α-glucosidase, CBD and THC exhibited best bounded conformation and interactions in the active binding site of α-glucosidase protein (Figs. 1 and 2). Therefore, they could be potentially used as therapeutic agents to manage type 2 DM. Summary of molecular docking results is presented in Table 1.

The constricted substrate binding site of the target protein is sited close to C-terminal, a confined region of beta strands of the catalytic domain, hence making the loop conformation towards N-terminal of the beta-stand domain and the active site is collectively composed of catalytic and beta-sheets domain residues (Roig-Zamboni et al., 2017). THC generated best bounded conformation at −7.5 kcal/mol (Fig. 1a), and potentially generated hydrogen bond (Fig. 1b). However, most of the active sites of the target protein are hydrophobic in nature. Thus, only one hydrogen bond is generated with the PRO194 residue of target

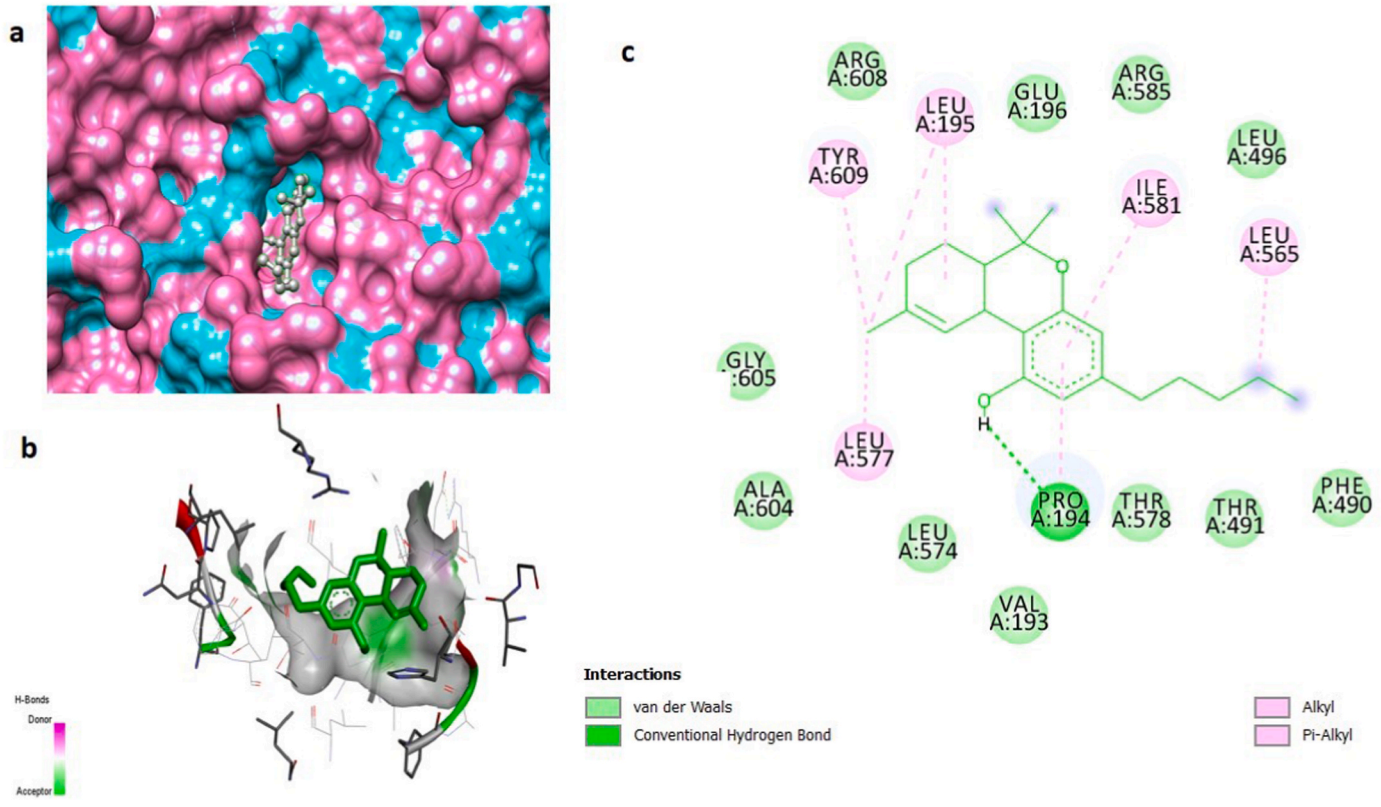

Fig. 1. Graphical representation of molecular docked complex of THC in the vicinity of active binding site of α-glucosidase protein (a), best bounded pose of THC presenting the potential of hydrogen bonding capacity (green presents hydrogen bond acceptor region, and purple presents the hydrogen bond donor region) with active binding site residues (b), and two-dimensional plot presenting binding interactions of the THC with target α-glucosidase protein (c). (For interpretation of the references to colour in this figure legend, the reader is referred to the Web version of this article.)

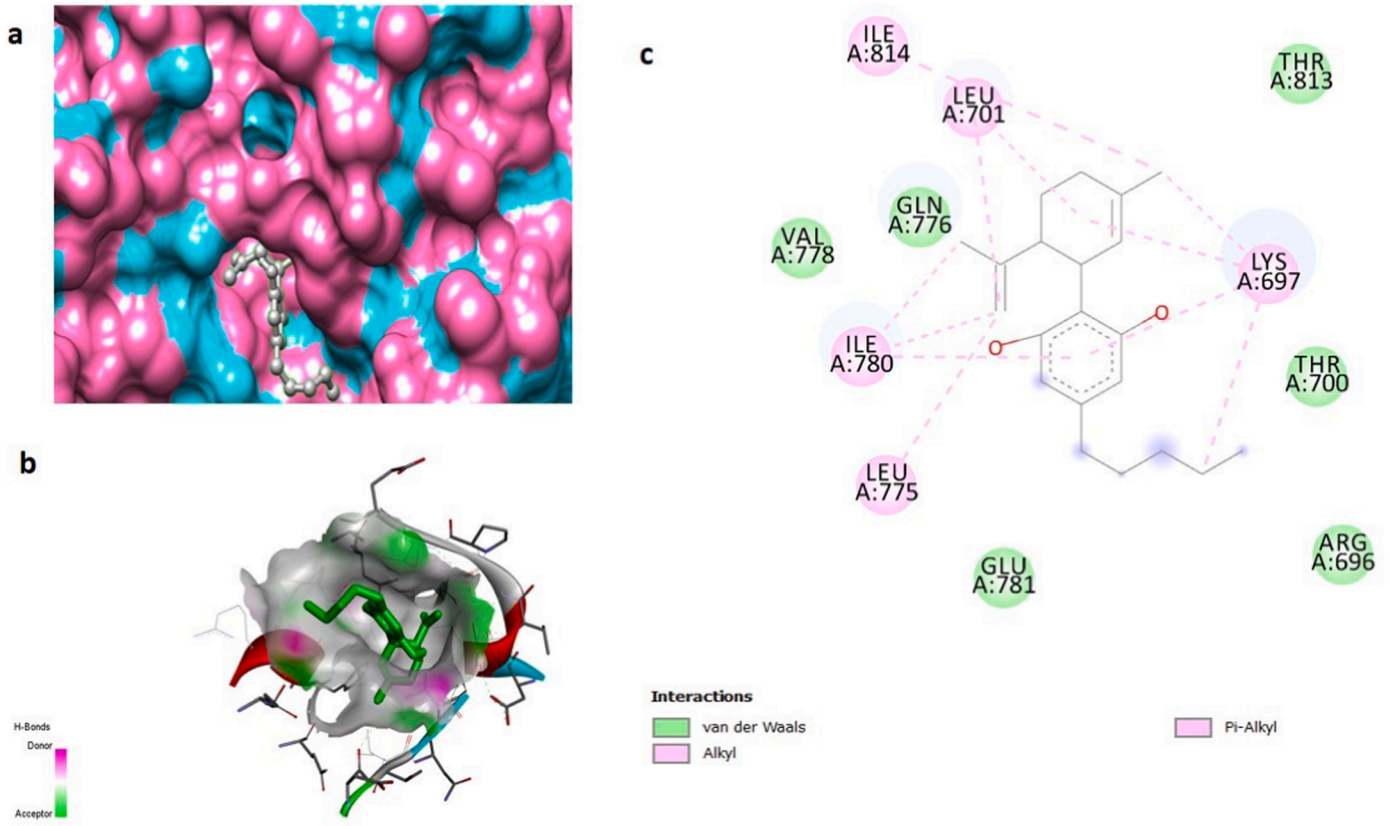

Fig. 2. Graphical representation of molecular docked complex of CBD in the vicinity of active binding site of α-glucosidase protein (a), best bounded pose of CBD presenting the potential of hydrogen bonding capacity (green presents hydrogen bond acceptor region, and purple presents the hydrogen bond donor region) with active binding site residues (b), and two-dimensional plot presenting binding interactions of the CBD with target α-glucosidase protein (c). (For interpretation of the references to colour in this figure legend, the reader is referred to the Web version of this article.)

Table 1
Summary of molecular docking results of THC and CBD with α-glucosidase target protein.

PubChem CID	Compounds	Binding energies (Kcal/mol)	Functional residues	Binding interactions
16078	THC	−7.5	VAL193, PRO194, LEU195, GLU196, PHE490, THR491, LEU496, LEU565, LEU574, LEU577, THR578, ILE581, ARG585, ALA604, GLY605, ARG608, TYR609	Van Der Waals, Hydrogen bonds, Alkyl, Pi-Alkyl
644019	CBD	−6.9	ARG696, LYS697, THR700, LEU701, ILE775, GLN776, VAL778, ILE780, GLU781, THR813, LUE814	Van Der Waals, Alkyl, Pi-Alkyl

protein. In addition, Van der Waals interaction network with VAL193, GLU196, PHE490, THR491, LEU496, LEU574, THR578, ARG585, ALA604, and ARG608 residues, as well as LEU195, LEU565, LEU577, ILE581, and TYR609 residues were involved in alkyl and Pi-alkyl interactions of THC (Fig. 1c). CBD also generated the best bounded conformation at −6.9 kcal/mol (Fig. 2a). In contrast, it exhibited far less potential to generate hydrogen bond (Fig. 2b). However, the two-dimensional plot revealed that Van der Waals interaction network with ARG696, THR700, GLN776, VAL778, GLU781, and THR813 residues as well as LYS697, LEU701, LEU775, ILE780, and ILE814 residues were involved in alkyl and Pi-alkyl interactions of CBD (Fig. 2c).

3.1.2. *Determination of Pharmacokinetic/ADMET profiles*

Various studies have explained the importance of pharmacokinetic/ADMET profile estimation for the screening of databases to identify potential drug-like and a lead-like compounds that could be better suited in the design and development of new drugs (Bibi and Sakata, 2017; Khan et al., 2022). ADMET profiles are calculated by SwissADME (Daina et al., 2017) and Datawarrior tools (Sander et al., 2015). Physicochemical properties of the selected compound, namely molecular weight (MW), partition coefficient (log P), hydrogen bond acceptor (HBA), hydrogen bond donor (HDB), total polar surface area (TPSA), molar refractivity (MR), and rotatable bond (RB) are important drug-like characteristics calculated for selected compounds. *In silico* ADMET profiles, including important drug-like characteristics, pharmacokinetics, drug-likeness, medicinal chemistry along with toxicity estimated for THC and CBD are summarized in Table 2.

Based on the drug-likeness theory, the physicochemical properties of THC and CBD were in the acceptable ranges without any violation (Lipinski, 2004). Their lipophilicity and water solubility classes exhibited very good outcomes, with gastrointestinal drug absorption (GI-DA) and blood brain barrier (BBB) permeability were in the range of acceptable pharmacokinetic parameters (Kimura and Higaki, 2002). Although both cannabinoids were not P-glycoprotein (P-gp) substrate, THC exhibited inhibitory potential on CYP2C19, CYP2C9 and CYP2D6, while CBD showed inhibitory potential on CYP2C19, CYP2C9, CYP2D6 and CYP3A4. THC and CBD also possessed good skin permeation, with Log Kp values of −3.27 and −3.59 cm/s, respectively. Regarding their medicinal chemistry, PAINS and Brenk alerts showed minor violations

Table 2
Summary of *in silico* ADMET profiles estimated for THC and CBD.

Descriptors	THC	CBD
Formula	$C_{21}H_{30}O_2$	$C_{21}H_{30}O_2$
Molecular weight (MW)	314.46 g/mol	314.46 g/mol
Number of rotatable bonds (RB)	4	6
Number of hydrogen bond acceptors (HBA)	2	2
Number of hydrogen bond donors (HBD)	1	2
Molar refractivity (MR)	97.91	99.85
Total polar surface area (TPSA)	29.46 Å^2	40.46 Å^2
Lipophilicity (Log P)	5.41	5.42
Water Solubility (Log S)	−5.93	−5.41
Solubility Class	Moderately soluble	Moderately soluble
Pharmacokinetics		
Gastrointestinal drug absorption (GI-DA)	GI-DA+	GI-DA+
Blood brain barrier (BBB) permeability	BBB+	BBB+
P-glycoprotein (P-gp) substrate	Non-substrate	Non-substrate
CYP1A2 inhibitor	Non-inhibitor	Non-inhibitor
CYP2C19 inhibitor	Inhibitor	Inhibitor
CYP2C9 inhibitor	Inhibitor	Inhibitor
CYP2D6 inhibitor	Inhibitor	Inhibitor
CYP3A4 inhibitor	Non-inhibitor	Inhibitor
Log Kp (skin permeation)	−3.27 cm/s	−3.59 cm/s
Drug-likeness		
Lipinski rule (MW ≤ 500, logP ≤5, HBD ≤5, HBA ≤10)	Acceptable	Acceptable
Veber rule (RB ≤ 10, TPSA ≤140)	Acceptable	Acceptable
Drug-likeness	Yes	Yes
Bioavailability score	0.55	0.55
Medicinal chemistry		
PAINS alert	No alerts	No alerts
Brenk alert	1 alert: isolated alkene	1 alert: isolated alkene
Lead likeness rule (250 ≤ MW ≤ 350, Log P ≤ 3.5, RB ≤ 7)	Not lead-like (Log P > 3.5)	Not lead-like (Log P > 3.5)
Synthetic accessibility	Highly accessible (4.27)	Highly accessible (4.05)
Toxicity estimation		
Mutagenic	No toxic effects	No toxic effects
Tumorigenic	No toxic effects	No toxic effects
Irritant	No toxic effects	No toxic effects
Reproductive	No toxic effects	No toxic effects

(Bibi and Sakata, 2017). Brenk alert exhibited one isolated alkene group for both cannabinoids, which suggested to improve before moving a drug to the next phase of development. In addition, THC and CBD were highly accessible synthesis with the scores of 4.27 and 4.05. The toxicity estimation revealed that THC and CBD exhibited low toxicity, which were completely in acceptable ranges, in terms of mutagenic, tumorigenic, irritant and reproductive effects (Table 2). Therefore, the present study indicated that THC and CBD have very good Pharmacokinetic/ADMET profiles that might be potentially considered as drug-like compounds.

3.2. Preparation of SCE-I and SCE-II

Leaf and inflorescence extracts of cannabis, namely SCE-I and SCE-II were prepared using a microwave extraction and standardized using an HPLC method to contain CBD of 2.5% w/w and THC of 1.9% w/w for SCE-I, and CBD of 4.5% w/w and THC of 6.9% w/w for SCE-II (Table 3). The content of CBD and THC in the inflorescence extract were higher than those in the leaf extract by 1.8 and 3.6 times, respectively. It has been reported that accumulation of cannabinoids in cannabis was highest in the inflorescences and modest in the leaves. THC content in the inflorescences (3.0–21.5%) were higher than in the leaves (0.26–2.69%). Likewise CBD content in the inflorescences (0.02–9.84%) were also higher than in the leaves (0.01–1.24%) (Richins et al., 2018). Variation of cannabinoid content usually depends on cannabis chemovars and cultivated area (Jin et al., 2020). A ratio of THC and CBD content has been used as an important tool for characterization of *C. sativa* chemotypes. Generally, three chemotypes including chemotype I or "THC dominant" (CBD/THC ratio <0.5), chemotype II or "intermediate type" (CBD/THC ratio between 0.5 and 3), and chemotype III or "CBD dominant" (CBD/THC ratio >3.0) have been described (Elzinga et al., 2015). Therefore, the cannabis used in this study that have CBD/THC ratios of 1.3 and 0.7 for SCE-I and SCE-II, respectively is categorized as a chemotype II or intermediate type cannabis.

Table 3
CBD and THC content of leaf (SCE-I) and inflorescence (SCE-II) extracts of *C. sativa*.

Extracts	CBD (% w/w)[a]	THC (% w/w)[a]
SCE-I	2.5 ± 0.09	1.9 ± 0.10
SCE-II	4.5 ± 0.02	6.9 ± 0.01

[a] Values are expressed as mean ± SD.

Although THC and CBD are basically non-polar molecules, partial polarity of the solvent used for their extraction is necessary due to the presence of alcohol group in the cannabinoid molecule (Lazarjani et al., 2021). Based on the solubility parameter theory, the δ-values of THC and CBD are 21–23 MPa$^{1/2}$. Ethanol with the δ-values of 25 MPa$^{1/2}$ was reported to be more effective in extracting cannabinoids than other solvents, including butane (15 MPa$^{1/2}$), N-heptane (15.4 MPa$^{1/2}$), supercritical carbon dioxide (0–21.8 MPa$^{1/2}$) and olive oil (16.8–17.7 MPa$^{1/2}$) (King, 2019). In addition, ethanol has been reported as a suitable solvent for extraction of cannabinoids due to it exhibited high extraction capacity and safety than other organic solvents, including petroleum ether, naphtha, hexane, acetone, and methanol (Romano and Hazekamp, 2013; Brighenti et al., 2017; Ubeed et al., 2022).

3.3. In vitro α-glucosidase inhibition activity

The results of *in vitro* α-glucosidase inhibitory effects of CBD, THC, SCE-I, SCE-II and acarbose are shown in Table 4. Five concentrations of CBD, THC and SCE-I in the ranges of 0.8–12.5 μg/ml were used to determine the IC_{50} values. The results revealed that amongst these, SCE-I exhibited the strongest inhibitory activity (IC_{50} of 1.2 μg/ml), followed by THC (IC_{50} of 3.0 μg/ml or 9.5 μM), and CBD (IC_{50} of 5.5 μg/ml or 17.5 μM), respectively, which were all markedly stronger than the standard drug, acarbose (IC_{50} of 488.6 μg/ml). It should be noted that determination of an IC_{50} value of SCE-II have to be performed using five lower concentrations in the ranges of 0.08 and 1.25 μg/ml, since it possessed markedly higher inhibitory activity than those three samples, with an IC_{50} value of 0.16 μg/ml.

The present study indicated that THC exhibited significantly stronger α-glucosidase inhibitory activity than CBD in *in vitro* assay along with slightly better binding energies with functional residues of the target protein, α-glucosidase. These findings agree with a report on *in vivo* studies, which proposed that THC may decrease enzyme activities involved in sugar metabolism, including α-glucosidase, β-glucuronidase, acid phosphatase and fructose-6-phosphatase (Chakravarty and Ghosh, 1981). Nevertheless, the investigation of α-glucosidase inhibitory effects

Table 4
α-Glucosidase inhibitory activities of THC, CBD and cannabis extracts.

Compounds/Extracts	IC_{50} (μg/ml)
THC	3.0 ± 0.37[a]
CBD	5.5 ± 0.28[b]
SCE-I	1.2 ± 0.62[c]
SCE-II	0.16 ± 0.01[d]
Acarbose	488.6 ± 10.23[e]

*Values with non-identical letters (a, b, c, d and e) are significantly different ($p < 0.05$).

of THC and CBD in animal model is still required.

Interestingly, our findings also indicated that the standardized ethanol extracts of inflorescences (SCE-II) and leaves (SCE-I) of cannabis possessed significantly stronger α-glucosidase inhibitory effect than their marker compounds, THC and CBD. Therefore, the extracts have greater potential to alleviate diabetes, since very low concentrations of CBD and THC are needed. This may be due to synergistic effects between the cannabinoids or entourage effects with the other phytochemicals, such as terpenoids and flavonoids, in the crude ethanol extracts. Recently, phytochemical composition of cannabis inflorescences has been identified and reported to contain approximately 15–20% cannabinoids, 1–2% terpenoids, and 0.1% flavonoids, while cannabis leaves contained lower levels of cannabinoids (1–2%), terpenoids (0.1–0.2%), but higher level of flavonoids (0.3–0.4%) (Jin et al., 2020). The most abundance of flavonoids in cannabis were quercetin, kaempferol, luteolin and apigenin, which have been reported to possess good α-glucosidase inhibitor activity, with the IC_{50} values of 15, 32, 46, and 82 μM, respectively (Proença et al., 2017). On the other hands, terpenoids that have been identified in cannabis, including limonene, α-terpineol α-terpinene, geraniol, and linalool exhibited weak α-glucosidase inhibitory effect (Wojtunik-Kulesza et al., 2019). Therefore, the synergistic effect might be mainly from interactions with the flavonoid compounds. However, further studies on identification of other active principles and their synergistic effect against α-glucosidase inhibitory activity are still needed.

4. Conclusion

Our findings suggest that the major active principles for α-glucosidase inhibitory effects of cannabis extracts are THC (IC_{50} of 9.5 μM) and CBD (IC_{50} of 17.5 μM) due to their major abundance and potent activity. However, the standardized extracts of inflorescences (SCE-II) and leaves (SCE-I) of cannabis possess higher inhibitory effect than their marker compounds suggesting the synergistic effects of phytochemicals in cannabis. In addition, SCE-II exhibited higher activity than SCE-I due to its high content of cannabinoids. Therefore, SCE-II and SCE-I are highly recommended as new α-glucosidase inhibitors for type 2 diabetes patients. However, high quality *in vivo* and clinical studies are still required to fully understand their efficacy and safety profiles.

CRediT authorship contribution statement

Wiwit Suttithumsatid: extraction, HPLC analysis, enzyme assay and writing the manuscript. **Muhammad Ajmal Shah:** molecular docking analysis and pharmacokinetic/ADMET profile, estimation and writing the manuscript. **Shabana Bibi:** molecular docking analysis and pharmacokinetic/ADMET profile estimation and writing the manuscript. **Pharkphoom Panichayupakaranant:** conceptualization of the research and methodology, project supervision and administration, writing the manuscript.

Declaration of competing interest

The authors declare that they have no known competing financial interests or personal relationships that could have appeared to influence the work reported in this paper.

Acknowledgments and funding

The authors wish to thank Dr. Fredrick Eze for assistance with English editing. This research did not receive any specific grant from funding agencies in the public, commercial, or not-for-profit sectors.

References

Alqahtani, A.S., Hidayathulla, S., Rehman, M.T., El-Gamal, A.A., Al-Massarani, S., Razmovski-Naumovski, V., Alqahtani, M.S., El-Dib, R.A., Al-Ajmi, M.F., 2020. Alpha-amylase and alpha-glucosidase enzyme inhibition and antioxidant potential of 3-oxolupenal and katononic acid isolated from *Nuxia oppositifolia*. Biomolecules 10, 61.

Bibi, S., Sakata, K., 2017. An integrated computational approach for plant-based protein tyrosine phosphatase non-receptor type 1 inhibitors. Curr. Comput. Aided Drug Des. 13, 319–335.

Brighenti, V., Pellati, F., Steinbach, M., Maran, D., Benvenuti, S., 2017. Development of a new extraction technique and HPLC method for the analysis of non-psychoactive cannabinoids in fibre-type *Cannabis sativa* L.(hemp). J. Pharm. Biomed. Anal. 143, 228–236.

Chakravarty, I., Ghosh, J., 1981. Influence of cannabis and delta-9-tetrahydrocannabinol on the biochemistry of the male reproductive organs. Biochem. Pharmacol. 30, 273–276.

Crocq, M.A., 2020. History of cannabis and the endocannabinoid system. Dialogues Clin. Neurosci. 22, 223–228.

Daina, A., Michielin, O., Zoete, V., 2017. SwissADME: a free web tool to evaluate pharmacokinetics, drug-likeness and medicinal chemistry friendliness of small molecules. Sci. Rep. 7, 42717.

Derosa, G., Maffioli, P., 2012. α-Glucosidase inhibitors and their use in clinical practice. Arch. Med. Sci. 8, 899–906.

DiNicolantonio, J.J., Bhutani, J., O'Keefe, J.H., 2015. Acarbose: safe and effective for lowering postprandial hyperglycaemia and improving cardiovascular outcomes. Open Heart 2, e000327.

Elzinga, S., Fischedick, J., Podkolinski, R., Raber, J.C., 2015. Cannabinoids and terpenes as chemotaxonomic markers in cannabis. Nat. Prod. Chem. Res. 3, 1–9.

Fathima, A.J., Murugaboopathi, G., 2019. Computer aided drug design for finding a therapeutics for dengue virus targets. Int. J. Innovative Technol. Explor. Eng. 9, 766–771.

Galicia-Garcia, U., Benito-Vicente, A., Jebari, S., Larrea-Sebal, A., Siddiqi, H., Uribe, K.B., Ostolaza, H., Martín, C., 2020. Pathophysiology of type 2 diabetes mellitus. Int. J. Mol. Sci. 21, 6275.

Horváth, B., Mukhopadhyay, P., Haskó, G., Pacher, P., 2012. The endocannabinoid system and plant-derived cannabinoids in diabetes and diabetic complications. Am. J. Pathol. 180, 432–442.

Hossain, U., Das, A.K., Ghosh, S., Sil, P.C., 2020. An overview on the role of bioactive α-glucosidase inhibitors in ameliorating diabetic complications. Food Chem. Toxicol. 145, 111738.

Ismail, E.M., Shantier, S.W., Mohammed, M.S., Musa, H.H., Osman, W., Mothana, R.A., 2021. Quinoline and quinazoline alkaloids against COVID-19: an in silico multitarget approach. J. Chem. 2021, 1–11.

Jadoon, K.A., Ratcliffe, S.H., Barrett, D.A., Thomas, E.L., Stott, C., Bell, J.D., O'Sullivan, S.E., Tan, G.D., 2016. Efficacy and safety of cannabidiol and tetrahydrocannabivarin on glycemic and lipid parameters in patients with type 2 diabetes: a randomized, double-blind, placebo-controlled, parallel group pilot study. Diabetes Care 39, 1777–1786.

Jin, D., Dai, K., Xie, Z., Chen, J., 2020. Secondary metabolites profiled in cannabis inflorescences, leaves, stem barks, and roots for medicinal purposes. Sci. Rep. 10, 1–14.

Khan, M.A.B., Hashim, M.J., King, J.K., Govender, R.D., Mustafa, H., Al-Kaabi, J., 2020. Epidemiology of type 2 diabetes – global burden of disease and forecasted trends. J. Epidemiol. Glob. Health. 10, 107–111.

Khan, M.S., Mehmood, B., Yousafi, Q., Bibi, S., Fazal, S., Saleem, S., Sajid, M.W., Ihsan, A., Azhar, M., Kamal, M.A., 2021. Molecular docking studies reveal rhein from rhubarb (*Rheum rhabarbarum*) as a putative inhibitor of ATP-binding cassette superfamily G member 2. Med. Chem. 17, 273–288.

Khan, M., Patujo, J., Mushtaq, I., Ishtiaq, A., Tahir, M.N., Bibi, S., Khan, M.S., Mustafa, G., Mirza, B., Badshah, A., 2022. Anti-diabetic potential, crystal structure, molecular docking, DFT, and optical-electrochemical studies of new dimethyl and diethyl carbamoyl-N, N′-disubstituted based thioureas. J. Mol. Struct. 1253, 132207.

Kim, S., Thiessen, P.A., Bolton, E.E., Chen, J., Fu, G., Gindulyte, A., Han, L., He, J., He, S., Shoemaker, B.A., 2016. PubChem substance and compound databases. Nucleic Acids Res. 44, D1202–D1213.

Kimura, T., Higaki, K., 2002. Gastrointestinal transit and drug absorption. Biol. Pharm. Bull. 25, 149–164.

King, J.W., 2019. The relationship between cannabis/hemp use in foods and processing methodology. Curr. Opin. Food Sci. 28, 32–40.

Lazarjani, M.P., Young, O., Kebede, L., Seyfoddin, A., 2021. Processing and extraction methods of medicinal cannabis: a narrative review. J. Cannabis Res. 3, 1–15.

Lipinski, C.A., 2004. Lead-and drug-like compounds: the rule-of-five revolution. Drug Discov. Today Technol. 1, 337–341.

Ma, H., Li, H., Liu, C., Seeram, N.P., 2021. Evaluation of cannabidiol's inhibitory effect on alpha-glucosidase and its stability in simulated gastric and intestinal fluids. J. Cannabis Res. 3, 1–6.

Proença, C., Freitas, M., Ribeiro, D., Oliveira, E.F., Sousa, J.L., Tomé, S.M., Ramos, M.J., Silva, A.M., Fernandes, P.A., Fernandes, E., 2017. α-Glucosidase inhibition by flavonoids: an in vitro and in silico structure–activity relationship study. J. Enzym. Inhib. Med. Chem. 32, 1216–1228.

Quattrocchi, E., Goldberg, T., Marzella, N., 2020. Management of type 2 diabetes: consensus of diabetes organizations. Drugs Context 9, 212607.

Richins, R.D., Rodriguez-Uribe, L., Lowe, K., Ferral, R., O'Connell, M.A., 2018. Accumulation of bioactive metabolites in cultivated medical Cannabis. PLoS One 13, e0201119.

Roig-Zamboni, V., Cobucci-Ponzano, B., Iacono, R., Ferrara, M.C., Germany, S., Bourne, Y., Parenti, G., Moracci, M., Sulzenbacher, G., 2017. Structure of human lysosomal acid α-glucosidase–a guide for the treatment of Pompe disease. Nat. Commun. 8, 1111.

Romano, L.L., Hazekamp, A., 2013. Cannabis oil: chemical evaluation of an upcoming cannabis-based medicine. Cannabinoids 1, 1–11.

Saingam, W., Sakunpak, A., 2018. Development and validation of reverse phase high performance liquid chromatography method for the determination of delta-9-tetrahydrocannabinol and cannabidiol in oromucosal spray from cannabis extract. Rev. Bras. Farmacogn. 28, 669–672.

Saleem, U., Bibi, S., Shah, M.A., Ahmad, B., Saleem, A., Chauhdary, Z., Anwar, F., Javaid, N., Hira, S., Akhtar, M.F., 2021a. Anti-Parkinson's evaluation of *Brassica juncea* leaf extract and underlying mechanism of its phytochemicals. Front. Biosci. (Landmark Ed). 26, 1031–1051.

Saleem, U., Shehzad, A., Shah, S., Raza, Z., Shah, M.A., Bibi, S., Chauhdary, Z., Ahmad, B., 2021b. Antiparkinsonian activity of *Cucurbita pepo* seeds along with possible underlying mechanism. Metab. Brain Dis. 36, 1231–1251.

Sander, T., Freyss, J., von Korff, M., Rufener, C., 2015. DataWarrior: an open-source program for chemistry aware data visualization and analysis. J. Chem. Inf. Model. 55, 460–473.

Shah, M.A., Khalil, R., Ul-Haq, Z., Panichayupakaranant, P., 2017. α-Glucosidase inhibitory effect of rhinacanthins-rich extract from *Rhinacanthus nasutus* leaf and synergistic effect in combination with acarbose. J. Funct.Foods 36, 325–331.

Suttithumsatid, W., Panichayupakaranant, P., 2020. Narrative review: phytocannabinoids and their potential use as a phytochemotherapy. Int. J. Pharmacogn. Chinese. Med. 4, 000209.

Trott, O., Olson, A.J., 2010. AutoDock Vina: improving the speed and accuracy of docking with a new scoring function, efficient optimization, and multithreading. J. Comput. Chem. 31, 455–461.

Ubeed, H.M.S.A., Bhuyan, D.J., Alsherbiny, M.A., Basu, A., Vuong, Q.V., 2022. A comprehensive review on the techniques for extraction of bioactive compounds from medicinal cannabis. Molecules 27.

Wojtunik-Kulesza, K.A., Kasprzak, K., Oniszczuk, T., Oniszczuk, A., 2019. Natural monoterpenes: much more than only a scent. Chem. Biodivers. 16, e1900434.

Wu, Y., Fu, R., Lei, C., Deng, Y., Lou, W., Wang, L., Zheng, Y., Deng, X., Yang, S., Wang, M., 2021. Estimates of type 2 diabetes mellitus burden attributable to particulate matter pollution and its 30-year change patterns: a systematic analysis of data from the global burden of disease study 2019. Front. Endocrinol. 12, 689079.